

Zigzag and Checkerboard Magnetic Patterns in Orbitally Directional Double-Exchange Systems

W. Brzezicki,^{1,2} C. Noce,¹ A. Romano,¹ and M. Cuoco¹

¹CNR-SPIN and Dipartimento di Fisica “E. R. Caianiello”, Università di Salerno, IT-84084 Fisciano (SA), Italy

²Marian Smoluchowski Institute of Physics, Jagellonian University, Reymonta 4, 30-059 Kraków, Poland

(Received 27 October 2014; revised manuscript received 15 April 2015; published 16 June 2015)

We analyze a t_{2g} double-exchange system where the orbital directionality of the itinerant degrees of freedom is a key dynamical feature that self-adjusts in response to doping and leads to a phase diagram dominated by two classes of ground states with zigzag and checkerboard patterns. The prevalence of distinct orderings is tied to the formation of orbital molecules that in one-dimensional paths make insulating zigzag states kinetically more favorable than metallic stripes, thus allowing for a novel doping-induced metal-to-insulator transition. We find that the basic mechanism that controls the magnetic competition is the breaking of orbital directionality through structural distortions, and highlight the consequences of the interorbital Coulomb interaction.

DOI: 10.1103/PhysRevLett.114.247002

PACS numbers: 74.70.Pq, 71.30.+h, 75.25.Dk, 75.30.-m

Transition metal (TM) oxides are fascinating materials characterized by a subtle interplay between charge, spin, and orbital degrees of freedom, which in many cases gives rise to complex types of collective behavior. Though first thought as a prerogative of $3d$ systems [1,2], this class of phenomena seems now to be ubiquitous in $4d$ and $5d$ ones [3,4]. A key role in their occurrence is played on one side by the frustrated localized-itinerant nature of the magnetic correlations, and on the other side by the peculiar orbital dependent electron dynamics in partially filled e_g and t_{2g} sectors of d shells. Prototype examples of electronic self-organization are provided by the magnetic and charge orders detected in layered manganites [5–7] and nickelates [8].

The formation of spin-charge density modulations is strongly related to the orbital character of the electronic system as demonstrated by the dominant role of lattice distortions in itinerant e_g systems [9–11] compared with the spin-orbital exchanges in models of insulating t_{2g} electrons [12,13]. More unexplored is the case of partially localized t_{2g} electrons in systems with low dimensionality and competing magnetic correlations. In this context, new phenomena have recently been observed and investigated in hybrid oxides with partial substitution of inequivalent TM ions [14–18]. Particularly fascinating are the Mn-doped layered Sr ruthenates that represent a paradigmatic example of nontrivial coupling between itinerant ferromagnetic (FM) and localized antiferromagnetic (AF) degrees of freedom [19,20] in the doped t_{2g} sector with a resulting metal-insulator transition (MIT) [20–23] and magnetic order [19,20,22,24–26] that are decoupled and robust over a large range of doping [21,22,25].

In this Letter, we show general features of orbitally directional double-exchange (DE) layered systems as a novel metal-to-insulator transition and two predominant

types of orderings within the phase diagram. The DE mechanism is known to be at the origin of itinerant ferromagnetism in e_g systems and, when the superexchange between localized spins is considered, to yield exotic magnetic structures [9,27–34] and other states based on electronic self-organization [11,35], whose stability often relies on additional microscopic couplings, and is confined to specific electron densities. In the orbitally directional DE system, we show that the formation of orbital molecules, within one dimensional (1D) FM configurations, is crucial to have insulating zigzag patterns that are energetically more favorable than metallic straight stripes, thus allowing for a novel kind of MIT. We find that, due to the orbital directionality, the competition between AF and FM correlations in layered systems makes antiferromagnetically coupled FM zigzag stripes and checkerboard clusters (Fig. 1) the dominant patterns in the phase diagram over a large range of doping. We demonstrate how the breaking of the orbital directionality as well as the inclusion of the Coulomb interaction can significantly affect the zigzag-checkerboard competition and lead to orbital or charge ordering in the ground state.

The model Hamiltonian is

$$\mathcal{H} = \sum_{i,\sigma} \sum_{\substack{\alpha,\beta=a,b \\ \hat{\gamma}=\hat{a},\hat{b},\hat{c}}} t_{\hat{\gamma},\alpha\beta} (d_{i,\alpha\sigma}^\dagger d_{i+\hat{\gamma},\beta\sigma} + \text{H.c.}) - J_H \sum_{i,\alpha=a,b} \mathbf{s}_{i\alpha} \cdot \mathbf{S}_i \\ + J_{AF} \sum_{i,\hat{\gamma}=\hat{a},\hat{b}} \mathbf{S}_i \cdot \mathbf{S}_{i+\hat{\gamma}} + U' \sum_i n_{i,a} n_{i,b},$$

where $d_{i,\alpha\sigma}^\dagger$ is the electron creation operator at the site i with spin σ for the orbital α . For convenience (a, b, c) indicate the (yz, xz, xy) orbitals which are perpendicular to the corresponding bond direction, with \hat{a} , \hat{b} , and \hat{c} being the unit vectors along the lattice symmetry directions. $n_{i,\alpha}$ is

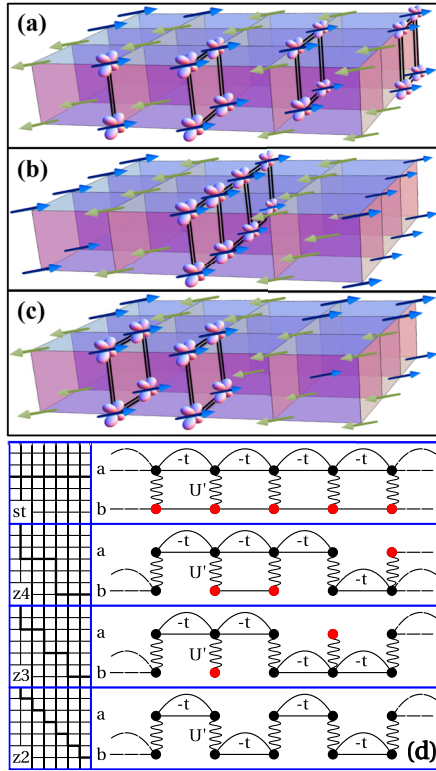


FIG. 1 (color online). Schematic view of layered t_{2g} systems with $d_{xz/yz}$ itinerant degrees of freedom and different antiferromagnetic and orbital patterns: (a) two-site segment zigzag z_2 (E phase), (b) straight stripes st , and (c) 2×2 -cell checkerboard c_2 . Doubled lines denote the constrained hopping for $d_{xz/yz}$ orbitals in undistorted systems. (d) sketch of the hoppings for embedded 1D paths (thick lines); stripe st and zigzag z_4 , z_3 , and z_2 phases. For each site there are two orbital flavors (dots) a and b , black (red) marks the active (inactive) orbitals. The arcs mark bonds where hopping is allowed. The structure is repeated in the second layer. The wiggly line denotes the on site interorbital coupling U' .

the local electron density for the orbital α , $s_{i\alpha} = \frac{1}{2} d_{i,\alpha,m}^\dagger \vec{\sigma}_{m,n} d_{i,\alpha,n}$ and S_i denote the spins for the $d_{xz/yz}$ and d_{xy} orbitals, respectively. $t_{\hat{\gamma},\alpha\beta}$ is the nearest-neighbor hopping amplitude between the orbitals α and β for the bond along the $\hat{\gamma}$. We take the tetragonal amplitudes $t_{\hat{a},bb} = t_{\hat{b},aa} = -t$ with t as energy scale unit. J_H stands for the Hund coupling between localized and itinerant electrons while J_{AF} is the AF superexchange of c orbitals. The hole doping x leads to $d_{xz/yz}^3 - d_{xz/yz}^2$ partial substitution. We consider that J_{AF} follows from virtual charge excitations in the presence of strong on site Coulomb interaction and we focus on the Hund coupling and the interorbital Coulomb interaction U' for the xz/yz orbitals. This assumption is also motivated by the connection between DE and orbital-selective-Mott physics [36–38]. To determine the ground state (GS) the local spins are considered as Ising variables [39].

We start by dealing with isolated 1D-FM paths in a two-dimensional (2D) layered structure for the undistorted

noninteracting case ($U' = 0$). The model (1) is solved for all the allowed 1D configurations made of straight stripe (st) and zigzag patterns (zn) with n -atom segments [Fig. 1(d)]. In the st case, one orbital is blocked and the other one is itinerant, while the zigzag has both orbitals active along the corresponding segments. The $d_{xz/yz}$ connectivity for the zigzag profiles can be mapped on a 1D view as reported in Fig. 1(d). For any zigzag, the GS is insulating and it factorizes in the product of orbital active electronic configurations within each segment. Because of the freedom of one or two itinerant channels, the issue is to determine which path lowers the kinetic energy when doping the system. In Fig. 2 we report the GS diagram as a function of doping and interlayer hopping $t_{\hat{c},aa/bb}$. We note that below half-filling ($x < 0.5$) the z_2 zigzag pattern is the dominant state, reflecting the general tendency, induced by doping, to avoid electron propagation along straight stripes.

To get more insight, it is instructive to compare the GS energy of z_2 and st at $x = 0$ and for the monolayer case. The st path has a total energy per site equal to $-4t/(2\pi)$. On the other hand, the z_2 ground state is made of disconnected two-atom clusters with filled bonding and empty antibonding configurations. Hence, the GS energy per site is equal to $-t$ and it is lower than that of the st configuration. The robustness of z_2 relies on the possibility to fill only bonding states and to avoid configurations with nodes in the confined segments. We argue that the st state is generally unstable towards the formation of a molecular configuration where electrons *condense* in the lowest energy state and tend to minimize the nodes in the quantum wave function.

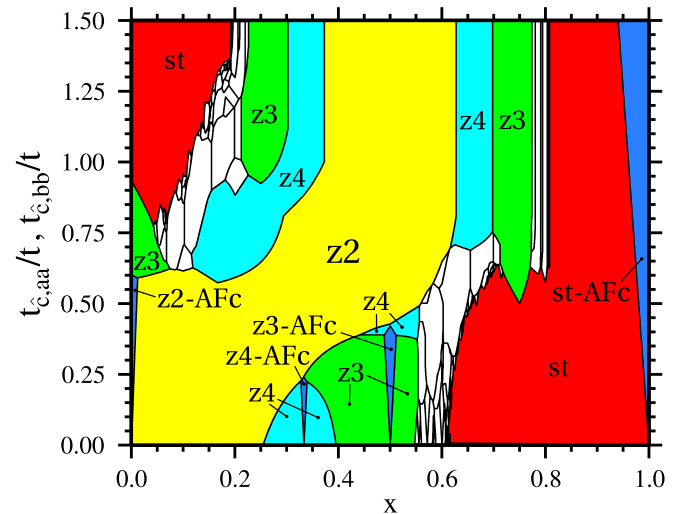


FIG. 2 (color online). Ground state diagram for embedded 1D FM patterns as a function of the hole doping x and the c -axis hoppings $t_{\hat{c},aa}$ and $t_{\hat{c},bb}$ at $U' = 0$. AFc denotes c -axis AF alignment. Unlabeled regions denote zn zigzag phases with $n > 4$.

A striking feature of the 1D diagram is that the doping-induced transition from metallic st to insulating $z2$ state goes through many intermediate zigzag configurations having long unit segments. This represents an unusual type of MIT with a breakdown of metallic paths into zigzag insulating ones. When considering the bilayer system, the flat orbitals acquire itinerancy along the interlayer direction [Fig. 1(a)] and compete with the in-plane $z2$ bonding. The result is the stabilization, at low and high doping, of larger zigzag configurations ($z3$ and $z4$) as well as straight stripes. We find that a change of the hopping amplitude around the doped site does not affect much the phase boundaries mostly due to the robust insulating character of the zn states.

In order to address the role of dimensionality we consider a double-layered system for a representative value of tetragonal anisotropy, i.e. $t_{\hat{c},aa(bb)} = 0.8t$. The results are obtained assuming the Hund coupling as the dominant energy scale, i.e., $J_H = 100t$. Smaller values of J_H (i.e., $J_H = 10t$ and $5t$) have also been considered and modify the diagram by reducing the area of stability of large size zn and cn patterns, slightly shifting the boundaries of the $z2$ and $c2$ phases. The search for spin patterns has been also performed in representative points of the diagram by means of Monte Carlo simulations employing the Metropolis algorithm. This analysis confirms the zigzag and checkerboard phases as the dominant ones. As shown in Fig. 3, FM and AF-FMc states occur at small and large J_{AF}

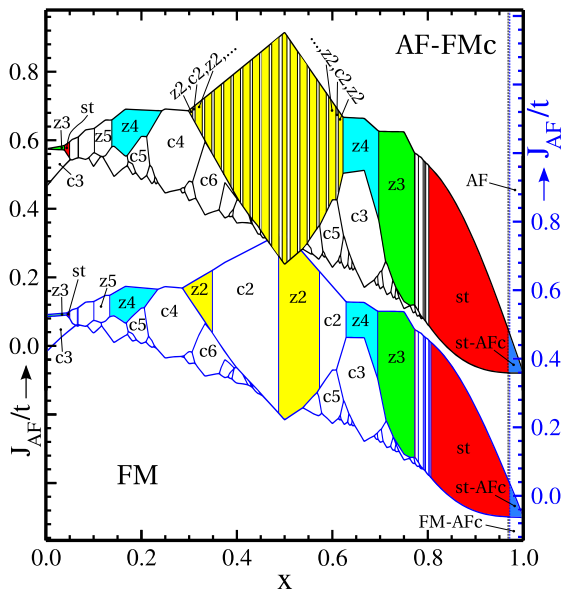


FIG. 3 (color online). Phase diagram of the 2D t_{2g} -DE model for the bilayered system vs doping x and J_{AF} , with no distortions, $U' = 0$ and in the presence of octahedral tilting angle θ : $\theta = 0^\circ$ (top side plot, left vertical scale) and $\theta = 10^\circ$ (bottom side plot, right vertical scale). FM and AF-FMc denote the FM and AF layers with FM c -axis alignment. The unlabeled regions are zn and cn phases with $n > 6$. The parameters used are at $\theta = 0$: $J_H = 100t$ and $t_{\hat{c},aa(bb)} = 0.8t$ (for $\theta = 10^\circ$, see Ref. [39]).

amplitudes. The AF-FMc is made of AF layers coupled ferromagnetically. The high doping regime, i.e., $x > 0.8$, exhibits a major tendency towards the st phase [Fig. 1(b)], which may be relevant for layered systems with hole-doped Mn^{4+} manganites or vanadates [40–42]. Since the d_{xy} band does not hybridize along the c direction, the effective AF coupling is vanishing and the interlayer ferromagnetism is always favored, except close to $x = 1$ due to the Pauli principle. As expected from the 1D study, the $z2$ zigzag states [Fig. 1(a)], are energetically favorable. However, they are quasidegenerate with checkerboard states (cn), made of $n \times n$ FM clusters that are coupled antiferromagnetically [Fig. 1(c) for the $c2$ configuration]. This result primarily arises from the fact the $z2$ and $c2$ electronic spectra are identical in the unit block due to the t_{2g} orbital directionality. The coupling between AF spin domains brings corrections of the order of $1/J_H$ in the dispersion and is responsible for the degeneracy removal and the cascade of doping induced transitions between $z2$ and $c2$. Rotation and tilting of the octahedra with respect to the c axis are the main processes that break the orbital directionality of the $d_{xz/yz}$ orbitals. To study their consequences we have employed a general approach based on the Slater-Koster rules [39,43]. The rotation does not modify the phase diagram boundaries because the hopping matrix transformation for the $d_{xz/yz}$ can be gauged away in the kinetic term. Then, it can only lead to transitions via a renormalization of J_{AF} . The tilting mixes $d_{xz/yz}$ orbitals [39] and thus breaks the directional disconnection resulting in the removal of the quasidegeneracy between the zigzag and checkerboard states (Fig. 3). The effects are more evident close to $x = 0.5$ where tilting favors the $c2$ state. Moreover, by reducing the interlayer diagonal hopping it makes $z2$ appearing at a lower doping down to $x \sim 0.3$ as in the 1D case.

We now discuss the role played by the U' interorbital Coulomb interaction [44–46]. We notice that U' is manifestly distinct for the zigzag and checkerboard patterns as due to the interplay of the pattern configuration and t_{2g} directionality. In the checkerboards, U' frustrates the confined $d_{xz/yz}$ charge motion in the spin-polarized blocks. On the contrary, in the zigzag there is an explicit difference for U' at the inner and the corner sites (Fig. 1). To deepen such comparison we focus on the tetragonal monolayer system. Inside the zigzag units one of the two orbitals is localized and the charge degree of freedom behaves like a classical variable. Then, the intrasegment interacting problem maps into the 1D Falicov-Kimball model [47] whose itinerant spinless electrons in the active $d_{xz/yz}$ orbitals locally couple to a classical variable describing the density of the inactive ones. At the corner sites, it is not possible to have a classical behavior and U' is fully quantum as the orbital electron density varies between zero and one depending on the intrasegment electronic configuration. The emerging low energy scenario is particularly clear for

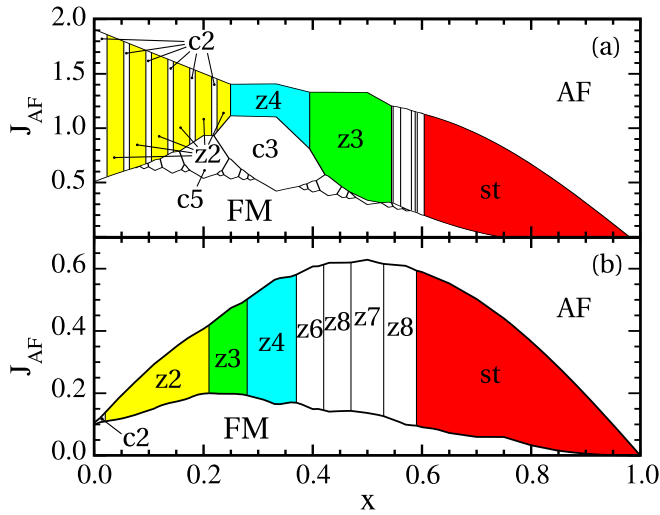


FIG. 4 (color online). Phase diagram of the monolayer tetragonal system with $U' = 0$ (a) and $U' = 10t$ (b).

the $z2$ state. One can show that the interacting problem can be exactly mapped into an Ising model in a transverse field. Then, the GS is made of domain walls that propagate along the zigzag path controlled by the ratio U'/t . Such modes generally allow for a kinetic energy gain. For larger zigzag patterns the intra-corner electronic separation leads to enhanced electron-hole correlations at the corner to avoid U' and the GS exhibits a tendency to an asymmetric charge distribution inside the zigzag block.

In order to quantitatively account for the role of U' we employ an exact diagonalization study based on the Lanczos algorithm, simulating both zigzag and checkerboard patterns with different cluster size [39]. In Fig. 4 we report the phase diagram for the 2D monolayer tetragonal system at $U' = 0$ (a) and $U' = 10t$ (b). A general outcome is that the intrablock kinetic energy is reduced by U' and increases its competition with the AF exchange. Such an aspect is particularly relevant for the stability of the checkerboard states as the AF energy contribution cancels out for all the zigzag states while, except for $c2$, it is detrimental for the checkerboard configurations. Then, the window of stability of the zigzag and checkerboard states shrinks in terms of the J_{AF}/t ratio. At low doping the competition is purely of electronic origin as the AF exchange is equivalent for the $z2$ and $c2$ states. It is worth pointing out how U' drives the stability of the $z2$ state. U' tends to kinetically frustrate the electron propagation for both $z2$ and $c2$ and this effect is quite strong at low doping. However, for $z2$ such constraint can be released by the propagation of the interorbital defects along the zigzag path. Such collective behavior is absent in the checkerboard $c2$ configuration. Approaching the range of doping where in the noninteracting limit longer zigzag and checkerboard states compete (e.g., $z3$, $z4$, and $c3$), we observe that U' favors the zigzag phases. This result is a cooperative effect

between U' and J_{AF} because the interaction renormalizes the kinetic energy and then the AF exchange can easily overcome the difference in the electronic contribution that makes the checkerboard patterns more favorable in the range of doping close to $x = 0.5$. Above half filling, the density of minority spins is quite dilute and the Coulomb interaction is not much relevant. Hence, the Coulomb interaction confirms the occurrence of a doping induced MIT moving from a very dilute metallic stripe ($x \sim 1$) to intermediate long zigzag ($x \sim 0.5$) and dense short zigzag patterns ($x \sim 0$) that is akin to an electronic gas-to-liquid-to-crystal changeover. A distinct feature occurs when considering the charge profile of the zigzag GS. We find that, among all the zigzags, the $z3$ state exhibits a GS with a charge density wave with nonuniform electron density. The correlated $z3$ phase has a charge and orbital ordering that remarkably can yield a nonvanishing electric dipole in each zigzag unit, making the single zigzag chain prone to a ferroelectric instability.

In summary, we have determined the spin-charge-orbital modulated patterns that naturally emerge in orbitally directional t_{2g} DE systems for an extended range of doping and couplings. We argue that these results can be of high relevance for understanding the phase diagram of Mn-doped layered Sr ruthenates or other oxides where TM substitutions can lead to d^3-d^4 or d^2-d^3 charge doping in the t_{2g} sector with a partial localization of one orbital degree of freedom.

We thank A. M. Oleś and R. Jin for valuable discussions. W. B. acknowledges support by the Polish National Science Center (NCN), Project No. 2012/04/A/ST3/00331, and the Foundation for Polish Science (FNP) within the START program.

-
- [1] M. Imada, A. Fujimori, and Y. Tokura, *Rev. Mod. Phys.* **70**, 1039 (1998).
 - [2] E. Dagotto, *Science* **309**, 257 (2005).
 - [3] B. J. Kim, H. Ohsumi, T. Komesu, S. Sakai, T. Morita, H. Takagi, and T. Arima, *Science* **323**, 1329 (2009).
 - [4] D. Pesin and L. Balents, *Nat. Phys.* **6**, 376 (2010).
 - [5] Y. Moritomo, Y. Tomioka, A. Asamitsu, Y. Tokura, and Y. Matsui, *Phys. Rev. B* **51**, 3297 (1995).
 - [6] B. J. Sternlieb, J. P. Hill, U. C. Wildgruber, G. M. Luke, B. Nachumi, Y. Moritomo, and Y. Tokura, *Phys. Rev. Lett.* **76**, 2169 (1996).
 - [7] Y. Tokura, *Rep. Prog. Phys.* **69**, 797 (2006).
 - [8] J. M. Tranquada, D. J. Buttrey, V. Sachan, and J. E. Lorenzo, *Phys. Rev. Lett.* **73**, 1003 (1994).
 - [9] T. Hotta, A. Feiguin, and E. Dagotto, *Phys. Rev. Lett.* **86**, 4922 (2001).
 - [10] T. Hotta and E. Dagotto, *Phys. Rev. Lett.* **92**, 227201 (2004).
 - [11] S. Dong, R. Yu, J.-M. Liu, and E. Dagotto, *Phys. Rev. Lett.* **103**, 107204 (2009).
 - [12] P. Wróbel and A. M. Oleś, *Phys. Rev. Lett.* **104**, 206401 (2010).

- [13] F. Krüger, S. Kumar, J. Zaanen, and J. van den Brink, *Phys. Rev. B* **79**, 054504 (2009).
- [14] T. F. Qi, O. B. Korneta, L. Li, K. Butrouna, V. S. Cao, X. Wan, P. Schlottmann, R. K. Kaul, and G. Cao, *Phys. Rev. B* **86**, 125105 (2012).
- [15] Y. Cao *et al.*, arXiv:1406.4978.
- [16] H. Lei, W.-G. Yin, Z. Zhong, and H. Hosono, *Phys. Rev. B* **89**, 020409(R) (2014).
- [17] C. Dhital *et al.*, *Nat. Commun.* **5**, 3377 (2014).
- [18] W. Brzezicki, A. M. Oleś, and M. Cuoco, *Phys. Rev. X* **5**, 011037 (2015).
- [19] J. E. Ortmann, J. Y. Liu, J. Hu, M. Zhu, J. Peng, M. Matsuda, X. Ke, and Z. Q. Mao, *Sci. Rep.* **3**, 2950 (2013).
- [20] R. Mathieu, A. Asamitsu, Y. Kaneko, J. P. He, X. Z. Yu, R. Kumai, Y. Onose, N. Takeshita, T. Arima, H. Takagi, and Y. Tokura, *Phys. Rev. B* **72**, 092404 (2005).
- [21] B. Hu, G. T. McCandless, V. O. Garlea, S. Stadler, Y. Xiong, J. Y. Chan, E. W. Plummer, and R. Jin, *Phys. Rev. B* **84**, 174411 (2011).
- [22] M. A. Hossain *et al.*, *Phys. Rev. B* **86**, 041102(R) (2012).
- [23] G. Panaccione *et al.*, *New J. Phys.* **13**, 053059 (2011).
- [24] D. Mesa, F. Ye, S. Chi, J. A. Fernandez-Baca, W. Tian, B. Hu, R. Jin, E. W. Plummer, and J. Zhang, *Phys. Rev. B* **85**, 180410(R) (2012).
- [25] M. A. Hossain *et al.*, *Sci. Rep.* **3**, 2299 (2013).
- [26] G. Li, Q. Li, M. Pan, B. Hu, C. Chen, J. Teng, Z. Diao, J. Zhang, R. Jin, and E. W. Plummer, *Sci. Rep.* **3**, 2882 (2013).
- [27] E. Dagotto, T. Hotta, and A. Moreo, *Phys. Rep.* **344**, 1 (2001).
- [28] S. Yunoki, T. Hotta, and E. Dagotto, *Phys. Rev. Lett.* **84**, 3714 (2000).
- [29] T. Hotta, M. Moraghebi, A. Feiguin, A. Moreo, S. Yunoki, and E. Dagotto, *Phys. Rev. Lett.* **90**, 247203 (2003).
- [30] S. Kumar, J. van den Brink, and A. P. Kampf, *Phys. Rev. Lett.* **104**, 017201 (2010).
- [31] D. J. Garcia, K. Hallberg, C. D. Batista, M. Avignon, and B. Alascio, *Phys. Rev. Lett.* **85**, 3720 (2000).
- [32] D. J. Garcia, K. Hallberg, C. D. Batista, S. Capponi, D. Poilblanc, M. Avignon, and B. Alascio, *Phys. Rev. B* **65**, 134444 (2002).
- [33] D. J. Garcia, K. Hallberg, B. Alascio, and M. Avignon, *Phys. Rev. Lett.* **93**, 177204 (2004).
- [34] H. Aliaga, B. Normand, K. Hallberg, M. Avignon, and B. Alascio, *Phys. Rev. B* **64**, 024422 (2001).
- [35] F. Ye, S. Chi, J. A. Fernandez-Baca, A. Moreo, E. Dagotto, J. W. Lynn, R. Mathieu, Y. Kaneko, Y. Tokura, and P. Dai, *Phys. Rev. Lett.* **103**, 167202 (2009).
- [36] L. de Medici, J. Mravlje, and A. Georges, *Phys. Rev. Lett.* **107**, 256401 (2011).
- [37] S. Biermann, L. de Medici, and A. Georges, *Phys. Rev. Lett.* **95**, 206401 (2005).
- [38] J. Rincón, A. Moreo, G. Alvarez, and E. Dagotto, *Phys. Rev. Lett.* **112**, 106405 (2014).
- [39] See Supplemental Material at <http://link.aps.org/supplemental/10.1103/PhysRevLett.114.247002> for details of the methodology, the numerical simulation, and the expressions of the effective hopping in terms of the rotation and tilting angles.
- [40] S. Miyasaka, T. Okuda, and Y. Tokura, *Phys. Rev. Lett.* **85**, 5388 (2000).
- [41] S. Ishihara, *Phys. Rev. Lett.* **94**, 156408 (2005).
- [42] K. Wohlfeld and A. M. Oleś, *Phys. Status Solidi B* **243**, 142 (2006).
- [43] J. C. Slater and G. F. Koster, *Phys. Rev.* **94**, 1498 (1954).
- [44] K. Held and D. Vollhardt, *Phys. Rev. Lett.* **84**, 5168 (2000).
- [45] M. J. Rozenberg, *Eur. Phys. J. B* **2**, 457 (1998).
- [46] D. I. Golosov, *Phys. Rev. Lett.* **104**, 207207 (2010).
- [47] L. M. Falicov and J. C. Kimball, *Phys. Rev. Lett.* **22**, 997 (1969).